



Combined effect of surface roughness and micropolar fluids on squeeze film characteristics between rough flat plate and curved annular plates

B.N. Hanumagowda¹, N. Chaithra², H.S. Doreswamy³ and A. Salma⁴

Abstract

The purpose of studying this paper is to investigate the combined impact of surface roughness and micropolar fluids on rough flat plate and curved annular plates by considering the squeezing action. Based on the micropolar fluid theory of Eringen and stochastic theory of Christensen's, the modified stochastic Reynolds equation is derived for the rough surface, using this equation pressure, load carrying capacity and squeeze film time are determined. From the results it is found that, the azimuthal (radial) roughness pattern increases (decreases) the pressure, load carrying capacity and squeeze film time.

Keywords

Curved annular plates, Micropolar fluids, Squeeze films, Surface roughness.

AMS Subject Classification: 376D08,74DXX,76E25.

^{1,4} School of Applied Sciences, REVA University, Bengaluru, Karnataka, India;

^{2,3} East Point College of Engineering and Technology, Bengaluru, Karnataka, India.

*Corresponding author: hanumagowda123@rediffmail.com;

Article History: Received 10 February 2020; Accepted 09 April 2020

©2020 MJM.

Contents

1	Introduction	570
2	Mathematical Formulation	571
3	Results and Discussion	572
3.1	Squeeze film pressure	573
3.2	Load carrying capacity	573
3.3	Squeeze film time	574
4	Conclusion	574
	References	574

1. Introduction

The analysis of micropolar fluid is studied by Eringen [1] and it is the subclass of microfluids. This fluid is widely used in industrial applications such as the solidification of liquid crystal, colloidal solution and exotic lubricants. Numerous studies are conducted using the micropolar fluid theory. Such as, the micropolar lubricant properties are studied by Maiti [2] in the reference of complex and step slider bearings. Isa and Zaheeruddin [3] shown that increasing the micropolar parameter, load supporting capacity and the time of approach increases and the friction coefficient decreases. In the presence

of micropolar fluid, bearing can support more load is analyzed by Agarwal *et al.* [4]. Many authors [5]-[12] have reported that in presence micropolar fluid lubricants load carrying capacity increases and friction coefficient decreases as compared with Newtonian case.

In recent years the study of the influence of surface roughness on different surfaces of bearings has received growing interest. This is mainly because of the reason that, in practice, most of the bearing surfaces are rough. Surface roughness is an important evaluation index of the quality of machine surface, which plays a significant role in reducing mechanical wear, impulsive damage and noise. The stochastic theory introduced by Christensen [13] to study the surface roughness effects in hydrodynamic lubrication, based on this analysis several authors studied the rough bearings. Shukla [14] analyzed the lubrication for rough surfaces and shown that the load carrying capacity increases with the values of roughness parameter increases. Prakash *et al.* [15] describe a theoretical analysis of squeeze film lubrication between two rough rectangular finite dimensional plates. Bujurke *et al.* [16] for curved annular plates and also Basti [17]. From their analysis it is found that surface roughness provides an improvement for pressure, load carrying capacity and lengthened squeeze film time.

The main purpose of studying this paper is to examine the micropolar fluids impacts on the rough flat plate and curved annular plates, no studies have been found in the literature. The present analysis is compared with smooth case studied by Hanumagowda *et al.*[10], and are presented in Table 1.

2. Mathematical Formulation

Figure 1 shows a squeeze film geometry in which upper plate is approaching towards lower plate with a normal velocity $V (= \frac{dh_m}{dt})$.

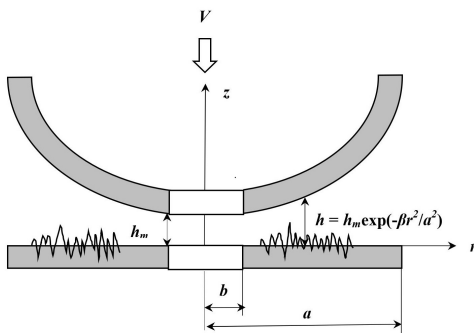


Figure 1: Squeeze film configuration of the rough flat plate and curved annular plate.

The film thickness h is defined as

$$h = h_m \exp(-\zeta r^2 / K^2); \quad k \leq r \leq K \quad (2.1)$$

Here h_m denotes the minimum film thickness, k and K are the inside and outside radii respectively, r is the radial coordinate and ζ is the curvature parameter.

The field equation for micropolar fluids are given by:

$$\left(\mu + \frac{\chi}{2}\right) \frac{\partial^2 u}{\partial z^2} + \chi \frac{\partial w_1}{\partial z} = \frac{\partial p}{\partial r} \quad (2.2)$$

$$\gamma \frac{\partial^2 w_1}{\partial z^2} - \chi \frac{\partial u}{\partial z} - 2\chi w_1 = 0 \quad (2.3)$$

$$\frac{1}{r} \frac{\partial}{\partial r} (ru) + \frac{\partial w}{\partial z} = 0 \quad (2.4)$$

where u and w are fluid velocity components and w_1 is the microrotational velocity component, χ is the spin viscosity, γ is the material coefficient and μ is the classical viscosity coefficient.

The significant boundary conditions are:

At the upper surface $z = h$

$$u = 0, \quad w_1 = 0, \quad w = \frac{dh_m}{dt} \quad (2.5)$$

At the lower surface $z = 0$

$$u = 0, \quad w_1 = 0, \quad w = 0 \quad (2.6)$$

The solution of the equations (2.2) and (2.3) are obtained by using the boundary conditions (2.5) and (2.6),

$$u = -\frac{p'}{\mu} \left\{ \frac{z^2}{2} - \frac{A^2 h}{m} \frac{(\cosh mz - 1)}{\sinh mh} \right\} + \frac{D}{(1-A^2)} \times \left\{ z - \frac{A^2}{m} \left(\sinh mz - (\cosh mz - 1) \frac{(\cosh mh - 1)}{\sinh mh} \right) \right\} \quad (2.7)$$

and

$$w_1 = \frac{D}{2(1-A^2)} (\cosh mz - 1) + \frac{\sinh mz}{\sinh mh} \times \left\{ \frac{hp'}{2\mu} - \frac{D}{2(1-A^2)} (\cosh mh - 1) \right\} - \frac{zp'}{2\mu} \quad (2.8)$$

where

$$m = \left(\frac{4\mu\chi}{\gamma(2\mu + \chi)} \right)^{1/2}, \quad A = \left(\frac{\chi}{2\mu + \chi} \right)^{1/2}, \quad D = \frac{-(1-A^2)}{2} \left(\frac{hp'}{\mu} \right), \quad B = \left(\frac{\gamma}{4\mu} \right)^{1/2}$$

Substituting u in the equation (2.4) and integrating we get,

$$\frac{1}{r} \frac{\partial}{\partial r} \left\{ Q(A, B, h) r \frac{\partial p}{\partial r} \right\} = 12\mu \frac{dh_m}{dt} \quad (2.9)$$

Where,

$$Q(A, B, h) = h^3 + 12B^2 h - 6ABh^2 \coth \left(\frac{Ah}{2B} \right), \quad m = \frac{A}{B}$$

The mathematical expression for film thickness to represent rough surface is considered as

$$H = h + h_s(r, \theta, \xi) \quad (2.10)$$

Taking stochastic average of (2.9), we get

$$\frac{1}{r} \frac{\partial}{\partial r} \left\{ E [Q(A, B, H)] r \frac{\partial E(p)}{\partial r} \right\} = 12\mu \frac{dh_m}{dt} \quad (2.11)$$

Where,

$$E(\bullet) = \int_{-\infty}^{\infty} (\bullet) g(h_s) dh_s \quad (2.12)$$

The probability distribution function $g(h_s)$ is given by;

$$g(h_s) = \begin{cases} \frac{35}{32n^7} (n^2 - h_s^2)^3 & -n < h_s < n \\ 0 & \text{elsewhere} \end{cases} \quad (2.13)$$

and h_s is the stochastic film thickness, $\bar{\sigma}$ is standard deviation and $n = 3\bar{\sigma}$.

The following two forms of roughness structures are considered in the context of Christensen [13] stochastic theory.

Radial Roughness

The roughness of this model is in the form of long, narrow



ridges and valleys running in r - direction and film thickness is denoted by

$$H = h + h_s(\theta, \xi)$$

Thus stochastic Reynolds equation (2.11) is written as:

$$\frac{1}{r} \frac{\partial}{\partial r} \left\{ E [Q(A, B, H)] r \frac{\partial E(p)}{\partial r} \right\} = 12\mu \frac{dh_m}{dt} \quad (2.14)$$

Azimuthal Roughness

The roughness of this model is in the form of long, narrow ridges and valleys running in θ - direction and film thickness is denoted by

$$H = h + h_s(r, \xi)$$

Thus stochastic Reynolds equation (2.11) is written as:

$$\frac{1}{r} \frac{\partial}{\partial r} \left\{ \frac{1}{E [1/Q(A, B, H)]} r \frac{\partial E(p)}{\partial r} \right\} = 12\mu \frac{dh_m}{dt} \quad (2.15)$$

Combining equations (2.14) and (2.15), we obtain

$$\frac{1}{r} \frac{\partial}{\partial r} \left\{ G(A, B, H, n) r \frac{\partial E(p)}{\partial r} \right\} = 12\mu \frac{dh_m}{dt} \quad (2.16)$$

where,

$$G(A, B, H, n) = \begin{cases} E [Q(A, B, H)] & \text{for radial roughness} \\ \{E [1/Q(A, B, H)]\}^{-1} & \text{for azimuthal roughness} \end{cases} \quad (2.17)$$

$$E [Q(A, B, H)] = \frac{35}{32n^7} \int_{-n}^n Q(A, B, H) (n^2 - h_s^2)^3 dh_s \quad (2.18)$$

$$E \left[\frac{1}{Q(A, B, H)} \right] = \frac{35}{32n^7} \int_{-n}^n \frac{(n^2 - h_s^2)^3}{Q(A, B, H)} dh_s \quad (2.19)$$

Using the following dimensionless variables in equation (2.15), we get

$$r^* = \frac{r}{K}, h^* = \frac{h}{h_{m0}} = h_m^* \exp(-\zeta r^{*2}), H^* = h^* + h_s^*, h_m^* = \frac{h_m}{h_{m0}}$$

$$h_s^* = \frac{h_s}{h_{m0}}, B^* = \frac{B}{h_{m0}}, P^* = \frac{E(p)h_{m0}^3}{\mu K^2(-dh_m/dt)}, c^* = \frac{n}{h_{m0}}$$

$$\frac{1}{r^*} \frac{\partial}{\partial r^*} \left\{ G^*(A, B^*, H^*, c^*) r^* \frac{\partial P^*}{\partial r^*} \right\} = -12 \quad (2.20)$$

where,

$$Q^*(A, B^*, H^*) = H^{*3} + 12B^{*2}H^* - 6AB^*H^{*2} \coth\left(\frac{AH^*}{2B^*}\right),$$

$$G^*(A, B^*, H^*, c^*) = \begin{cases} E [Q^*(A, B^*, H^*)] & \text{for radial roughness} \\ \{E [1/Q^*(A, B^*, H^*)]\}^{-1} & \text{for azimuthal roughness} \end{cases}$$

The pressure boundary conditions are:

$$P^* = 0 \quad \text{at} \quad r^* = k^* = k/K \quad (2.21)$$

$$P^* = 0 \quad \text{at} \quad r^* = 1 \quad (2.22)$$

The non-dimensional squeeze film pressure is obtained by integrating the equation (2.20) using the conditions (2.21) and (2.22),

$$P^* = \frac{6 \{J_1(1)J_2(r^*) - J_2(1)J_1(r^*)\}}{J_2(1)} \quad (2.23)$$

where,

$$J_1(r^*) = \int_{k^*}^{r^*} \frac{r^*}{G^*(A, B^*, H^*, c^*)} dr^*, \quad J_2(r^*) = \int_{k^*}^{r^*} \frac{1}{r^* G^*(A, B^*, H^*, c^*)} dr^*,$$

$$J_1(1) = \int_{k^*}^1 \frac{r^*}{G^*(A, B^*, H^*, c^*)} dr^*, \quad J_2(1) = \int_{k^*}^1 \frac{1}{r^* G^*(A, B^*, H^*, c^*)} dr^*$$

The load carrying capacity is obtained by integrating film pressure over the film region:

$$W = \int_{r=k}^K 2\pi r p dr \quad (2.24)$$

The dimensionless load carrying capacity is given by

$$W^* = \frac{E(W)h_{m0}^3}{2\pi\mu K^4(-dh_m/dt)} = \frac{6 \{J_1(1) \int_{k^*}^1 J_2(r^*) r^* dr^* - J_2(1) \int_{k^*}^1 J_1(r^*) r^* dr^*\}}{J_2(1)} \quad (2.25)$$

The dimensionless squeeze film time is given by

$$T^* = \frac{E(W)h_{m0}^3}{\pi\mu K^4} t = 12 \int_{h_m^*}^1 \left\{ \frac{J_1(1) \int_{k^*}^1 J_2(r^*) r^* dr^* - J_2(1) \int_{k^*}^1 J_1(r^*) r^* dr^*}{J_2(1)} \right\} dh_m^* \quad (2.26)$$

3. Results and Discussion

The combined impact of surface roughness and micropolar fluids on the squeeze film lubrication between rough flat plate and curved annular plate is studied by considering various non-dimensional parameters such as roughness parameter c^* , coupling number A , couple stress parameter B^* and curvature parameter ζ . As the roughness parameter $c^* \rightarrow 0$ the squeeze film characteristics analyzed in the current analysis reduces to the smooth case studied by Hanumagowda *et al.*[10]. The following set of values are considered in the present analysis $A = 0.0, 0.2, 0.4; B^* = 0.0, 0.05, 0.1; \zeta = -0.5, 0.0, 0.5$ and $c^* = 0.0, 0.1, 0.2$.

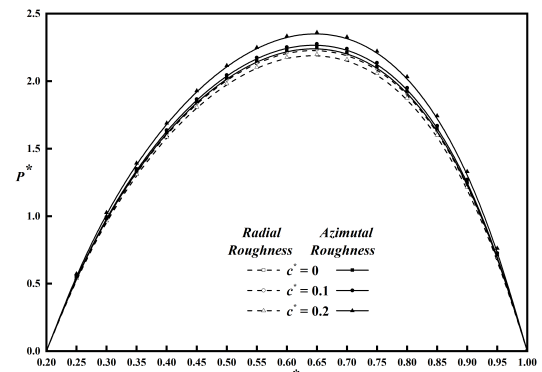


Figure 2: Plot of P^* versus r^* with $A = 0.2, B^* = 0.3, \zeta = 0.5$ and $k^* = 0.2$ for distinct values of c^*



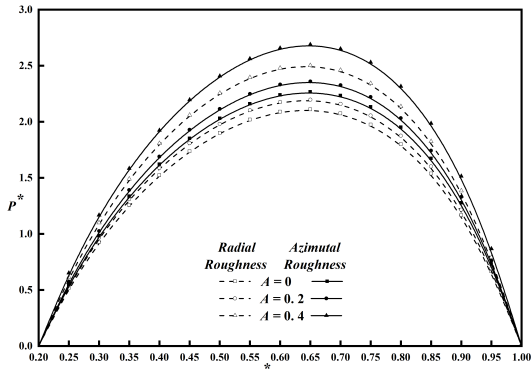


Figure 3: Plot of P^* versus r^* with $c^* = 0.2$, $B^* = 0.3$, $\zeta = 0.5$ and $k^* = 0.2$ for distinct values of A .

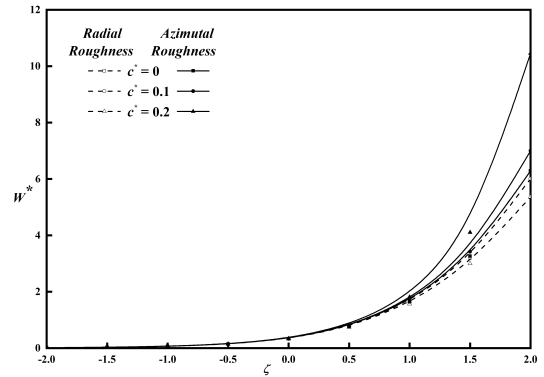


Figure 6: Plot of W^* versus ζ with $A = 0.2$, $B^* = 0.3$ and $k^* = 0.2$ for distinct values of c^* .

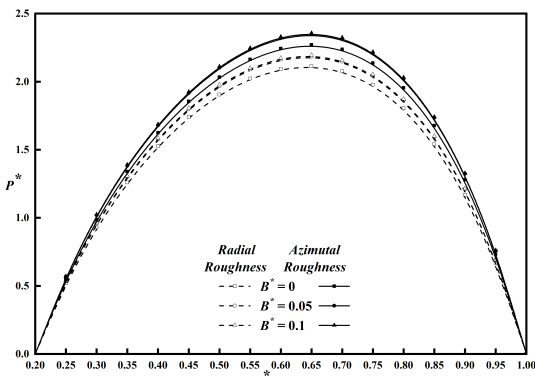


Figure 4: Plot of P^* versus r^* with $A = 0.2$, $c^* = 0.2$, $\zeta = 0.5$ and $k^* = 0.2$ for distinct values of B^* .

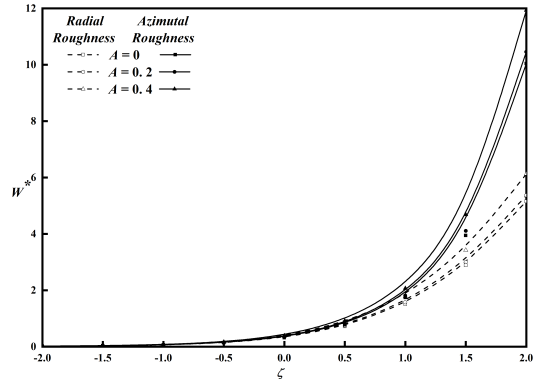


Figure 7: Plot of W^* versus ζ with $c^* = 0.2$, $B^* = 0.3$ and $k^* = 0.2$ for distinct values of A .

3.1 Squeeze film pressure

The deviation of dimensionless pressure P^* versus r^* as function of c^* is illustrated in Figure 2 with $A = 0.2$, $B^* = 0.3$, $\zeta = 0.5$ and $k^* = 0.2$ and it is found that for increasing values of c^* , pressure P^* increases (decreases) for azimuthal (radial) roughness patterns and also it is noticed that at $c^* = 0$ both the roughness patterns reduces to smooth case. The plot of P^* versus r^* for distinct values of A , B^* and ζ is shown in the Figure 3, 4 and 5 respectively and it is found that P^* significantly increases for larger values of A , B^* and ζ for both the roughness patterns.

3.2 Load carrying capacity

In Figure 6, the graph of non-dimensional load W^* as a function of ζ with $A = 0.2$, $B^* = 0.3$ and $k^* = 0.2$ for distinctive values of c^* is elaborated and it is noticed that for increasing the values of c^* , load W^* also increases for azimuthal and decreases for radial roughness patterns and when $c^* = 0$ both the roughness patterns reduces to smooth case. The graph of W^* against ζ for distinctive values of A and B^* is presented in Figure 7 and 8 respectively and it is seen that load carrying capacity W^* increases for increasing the values of A and B^* for both the roughness patterns.

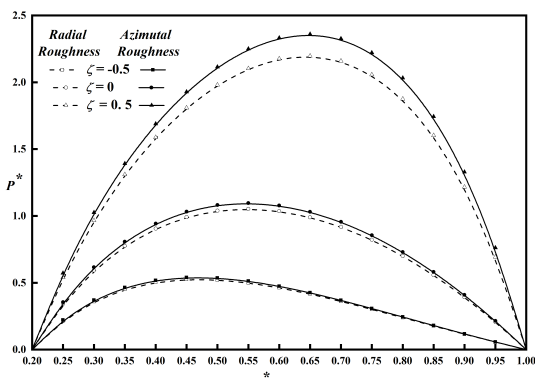


Figure 5: Plot of P^* versus r^* with $A = 0.2$, $c^* = 0.2$, $B^* = 0.3$ and $k^* = 0.2$ for distinct values of ζ .

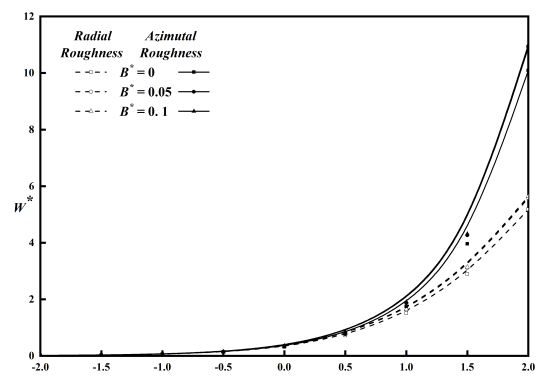


Figure 8: Plot of W^* versus ζ with $A = 0.3$, $c^* = 0.2$ and $k^* = 0.2$ for distinct values of B^* .



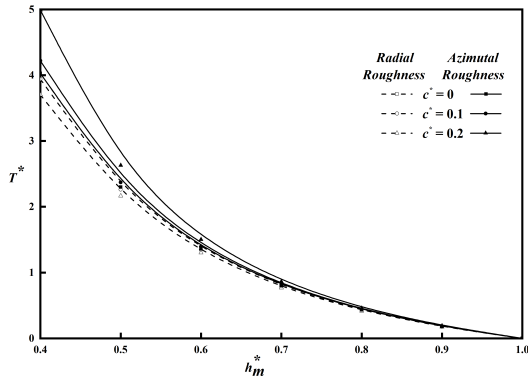


Figure 9: Plot of T^* versus h_m^* with $A = 0.2$, $B^* = 0.3$, $k^* = 0.2$ and $\zeta = 0.5$ for distinct values of c^* .

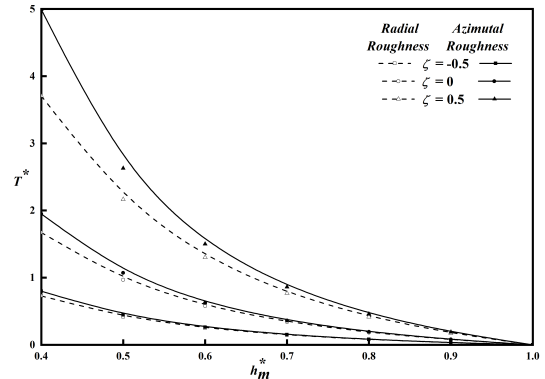


Figure 12: Plot of T^* versus h_m^* with $c^* = 0.2$, $A = 0.2$, $B^* = 0.3$ and $k^* = 0.2$ for distinct values of ζ .

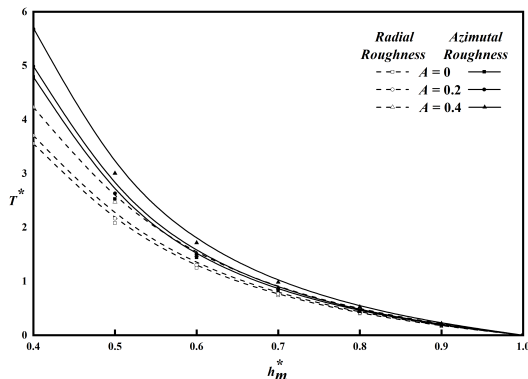


Figure 10: Plot of T^* versus h_m^* with $c^* = 0.2$, $B^* = 0.3$, $k^* = 0.2$ and $\zeta = 0.5$ for distinct values of A .

3.3 Squeeze film time

The graph of dimensionless squeeze film time T^* for distinct values of c^* against h_m^* is elaborated in Figure 9 and it shows that for larger values of c^* , T^* also increases (decreases) for azimuthal (radial) roughness patterns and from the figure it is clear that at $c^* = 0$ both the roughness patterns reduces to smooth case. The variation of T^* along h_m^* as function of A, B^* and ζ is presented in the Figure 10, 11 and 12 respectively and as the result, squeeze film time T^* increases for increasing values of A, B^* and ζ for both the roughness patterns.

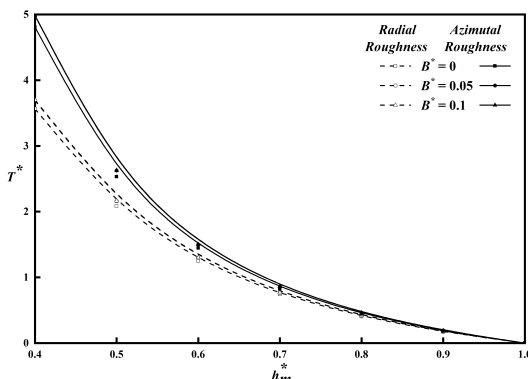


Figure 11: Plot of T^* versus h_m^* with $A = 0.2$, $c^* = 0.2$, $k^* = 0.2$ and $\zeta = 0.5$ for distinct values of B^* .

4. Conclusion

The impact of roughness and micropolar fluids on squeeze film characteristics between rough flat plate and curved annular plates is analysed. From the obtained results and discussion, the following conclusion can be drawn:

- Surface roughness has substantial influence on fluid squeeze film pressure, load carrying capacity and squeeze time as compared with smooth case discussed by Hanumagowda *et al.*[10].
- The presence of micropolar fluids enhances the pressure, load-carrying capacity and squeeze film time as compared to the corresponding Newtonian case.
- The squeeze film characteristic is significant for larger values of ζ .

Table 1: Comparison of present analysis with Hanumagowda *et al.*[10].

	Hanumagowda <i>et al.</i> [10]		Present analysis				
	$B^* = 0$	$B^* = 0.05$	$c^* = 0, B^* = 0$	$c^* = 0, B^* = 0.05$	$c^* = 0.2, B^* = 0$	$c^* = 0.2, B^* = 0.05$	
P^*	0	7.1998	7.1998	7.1998	6.8126	8.1413	
	0.2	7.2170	7.4798	7.2170	7.4798	6.8283	8.1626
	0.4	7.2347	8.2573	7.2347	8.2573	6.8444	8.1844
	0.6	7.2525	9.4829	7.2525	9.4829	6.8605	8.2064
W^*	0	3.4012	3.4012	3.4012	3.4012	3.1856	3.9440
	0.2	3.4101	3.5348	3.4101	3.5348	3.1936	3.9554
	0.4	3.4192	3.9181	3.4192	3.9181	3.2017	3.9672
	0.6	3.4284	4.5488	3.4284	4.5488	3.2100	3.9791
T^*	0	2.7209	2.7209	2.7209	2.7209	2.5485	3.1552
	0.2	2.7280	2.8278	2.7280	2.8278	2.5549	3.1643
	0.4	2.7353	3.1345	2.7353	3.1345	2.5614	3.1738
	0.6	2.7427	3.6390	2.7427	3.6390	2.5680	3.1833

References

- [1] A.C.Eringen., Theory of micropolar fluids, *J. Math. Mech.*, 16(1966), 1-18.
- [2] G.Maiti., Composite and step slider bearings in micropolar fluids, *Japanese J. Appl. Physics*, 12(7)(1973), 1058-64.
- [3] M.Isa and K. H.Zaheeruddin., Micropolar fluid lubrication of one-dimensional journal bearings, *Wear*, 50(2000), 211-220.
- [4] V.K. Agrawal and S B.Bhatt., Porous pivoted slider bearings lubricated with a micropolar fluid, *Wear*, 61(1)(1980), 1-8.
- [5] M.M.Khonsari and D. E.Brewer., On the performance of



- finite journal bearings lubricated with micropolar fluids, *Tri. Trans.*, 32(1989), 155-160.
- [6] N.B.Naduvanamani and A.Siddanagouda, Porous inclined stepped composite bearings with micropolar fluid, *Tribology Materials, Surfaces and Interfaces*, 1(4)(2007), 224-232.
- [7] N.B.Naduvanamani and G.B.Marali., Dynamicreynolds equation for micropolar fluid and the analysis of plane inclined slider bearings with squeezing effect, *J of Engg. Tribol.*, 221(7)(2007), 823-829.
- [8] N.B.Naduvanamani and S.S.Huggi., Micropolar fluid squeeze film lubrication of short partial porous journal bearings, *Proceedings of the Institution of Mechanical Engineers J*, 223(8)(2009), 1179–1185.
- [9] N.B.Naduvanamani and S.Santosh., Micropolar fluid squeeze film lubrication of finite porous journal bearing, *Tribol. International*, 44(4)(2011), 409-416.
- [10] B.N.Hanumagowda.,N. Chaithra and A.Salma., Effect of micropolar fluids on squeeze film lubrication between curved annular plates, *Journal of Physics*, 1000(2018), 1-8.
- [11] A.Siddangouda., Squeezing Film Characteristics for Micropolar fluid between Porous Parallel Stepped Plates, *Tribology in Industry*, 37(1)(2015), 97-106.
- [12] N.B.Naduvanamani and K.K.Archana., Effect of viscosity variation on the micropolar fluidsqueeze film lubrication of a short journal bearing, *Advances in Tribol.*, (2013), 1-7.
- [13] H.Christensen., Stochastic models for hydrodynamic lubrication of rough surfaces, *Proceedings of the Institution of Mechanical Engineers*, 184(1970), 1013–1026.
- [14] J.B.Shukla., A new theory of lubrication for rough surfaces, *Wear*, 49(1978), 33-42.
- [15] J.Prakash and H.Christensen., Squeeze films between two rough rectangular plates, *Journal of Mechanical Engineering Science*, 20(4)(1978), 183–188.
- [16] N.M.Bujurke., N.B.Naduvanamani and D.P.Basti., Effect of surface roughness on the squeeze film lubrication between curved annular plates, *Industrial Lubrication and Tribology*, 59(4)(2007), 178–185.
- [17] Dhanapal P Basti., Effect of surface roughness and couple stresses on squeeze films between curved annular plates, *ISRN Tribology*, 2013(2013), 1-8.

ISSN(P):2319 – 3786
Malaya Journal of Matematik
ISSN(O):2321 – 5666

